Atmospheric chemistry and aerosols

Sulcanese et al. (2024)

nature astronomy

Article

https://doi.org/10.1038/s41550-024-02272-1

Evidence of ongoing volcanic activity on Venus revealed by Magellan radar

Received: 21 March 2023

Accepted: 11 April 2024

Davide Sulcanese [1,2], Giuseppe Mitri [1,2] & Marco Mastrogiuseppe [3,4]

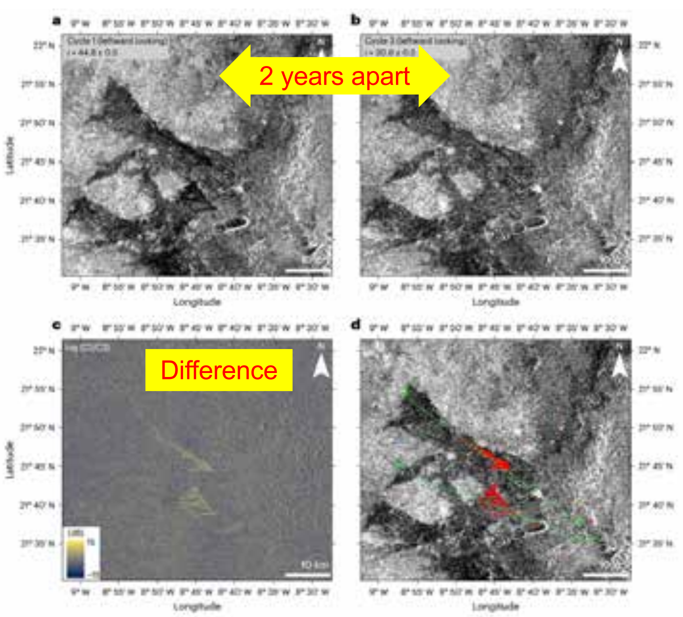

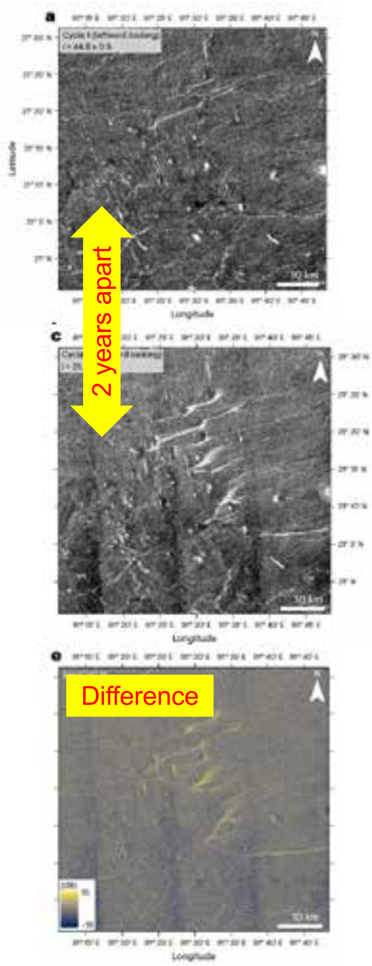

Composition of planetary atmospheres

Object	Mass (kilograms)	Carbon Dioxide	Nitrogen	Oxygen	Argon	Methane	Sodium	Hydrogen	Helium	Other
Sun	3.0×10^{30}							71%	26%	3%
Mercury	1000			42%			22%	22%	6%	8%
Venus	4.8×10^{20}	96%	4%							
Earth	1.4×10^{21}		78%	21%	1%					<1%
Moon	100,000				70%		1%		29%	
Mars	2.5×10^{16}	95%	2.7%		1.6%					0.7%
Jupiter	1.9×10^{27}							89.8%	10.2%	
Saturn	5.4×10^{26}							96.3%	3.2%	0.5%
Titan	9.1×10^{18}		97%			2%				1%
Uranus	8.6×10^{25}					2.3%		82.5%	15.2%	
Neptune	1.0×10^{26}					1.0%		80%	19%	
Pluto	1.3×10^{14}	8%	90%			2%				

from NASA HP

photosynthesis

$$6\,CO_2 + 6H_2O + \text{energy} \longrightarrow C_6H_{12}O_6 + 6\,O_2$$

Chemical kinetics

A reaction between reactants A and B to form product C:

A + B → C reaction rate = k [A] [B]

A + B + M → C + M reaction rate = k [A] [B] [M]

M is any inert molecule that can remove the excess energy.

k is the reaction rate constant that usually depends on the temperature as (Arrhenius equation):

$$k = A \exp\left(-\frac{E_a}{k_B T}\right)$$

where E_a is the activation energy.

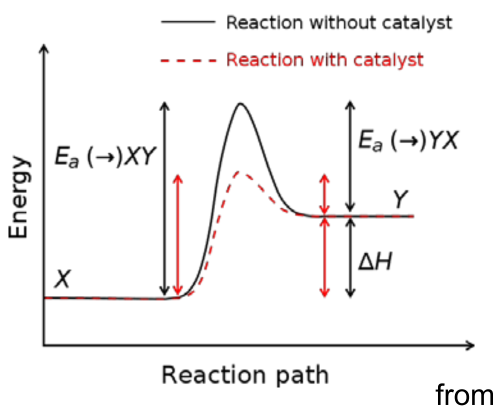

from Wikipedia

Production and destruction of ozone

Chapman theory

$O_2 + h\nu \rightarrow 2O$
$O + O_2 + M \rightarrow O_3 + M$

$3O_2 \rightarrow 2O_3$

$O_3 + h\nu \rightarrow O + O_2$
$O + O_3 \rightarrow 2O_2$

$2O_3 \rightarrow 3O_2$

- Chapman theory predicts an ozone amount of several times larger than the observations.
- Other loss mechanisms are required.

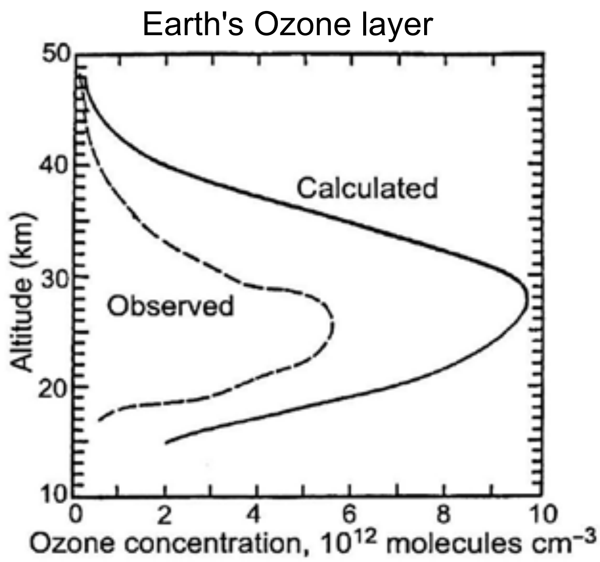

Figure 3.1 An ozone profile calculated with the Chapman reactions at the equator overestimates the ozone compared with observations over Panama at 9° N on November 13, 1970. The reason is that natural catalysts that destroy ozone are omitted from the oxygen-only Chapman reactions. (Adapted from Seinfeld and Pandis (1998). Reproduced with permission. Copyright 1998, John Wiley and Sons.)

Catling & Kasting (2017)

Catalytic cycles

$X + O_3 \rightarrow XO + O_2$
$XO + O \rightarrow X + O_2$

$O + O_3 \rightarrow 2O_2$

X : Free radical such as OH, NO, Cl, Br

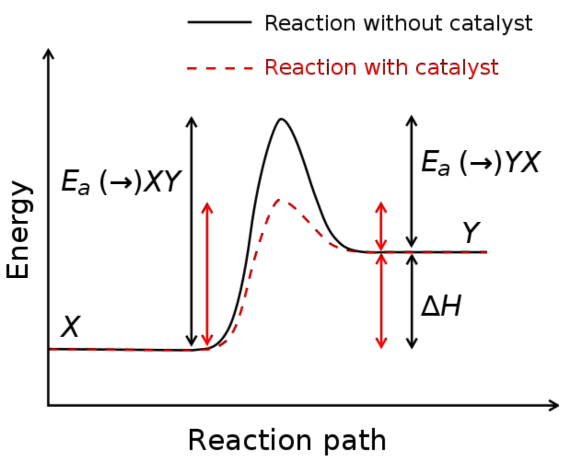

The net result of the catalytic cycle is to remove O and O_3 rapidly.

Stability of CO_2 atmosphere

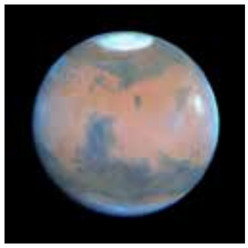

$$
\begin{aligned}
&2(CO_2 + h\nu \rightarrow CO + O) \\
&O + O + M \rightarrow O_2 + M \\
\hline
&\text{Net: } 2CO_2 \rightarrow 2CO + O_2
\end{aligned}
$$

The reaction CO + O → CO_2 is very slow (spin forbidden).
Mars and Venus atmospheres are expected to be converted to CO and O_2 in 6000 years.

Catalytic cycle on Mars ?

On Mars, OH radicals are thought to play crucial roles.

$$H_2O + h\nu \rightarrow OH + H$$

McElroy and Donahue [1972]

Production of OH

$$
\begin{aligned}
&H + O_2 + M \rightarrow \boxed{HO_2} + M \\
&\boxed{HO_2} + O \rightarrow \boxed{OH} + O_2
\end{aligned}
$$

Production of CO_2

$$CO + \boxed{OH} \rightarrow CO_2 + H,$$

Net reaction

$$CO + O + M \rightarrow CO_2 + M.$$

Parkinson and Hunten [1972]

Production of OH

$$
\begin{aligned}
&2(H + O_2 + M \rightarrow \boxed{HO_2} + M) \\
&\boxed{HO_2} + \boxed{HO_2} \rightarrow \boxed{H_2O_2} + O_2 \\
&\boxed{H_2O_2} + h\nu \rightarrow \boxed{OH} + OH
\end{aligned}
$$

Production of CO_2

$$2(CO + \boxed{OH} \rightarrow CO_2 + H),$$

Net reaction

$$2CO + O_2 \rightarrow 2CO_2.$$

Atreya and Gu (1994)

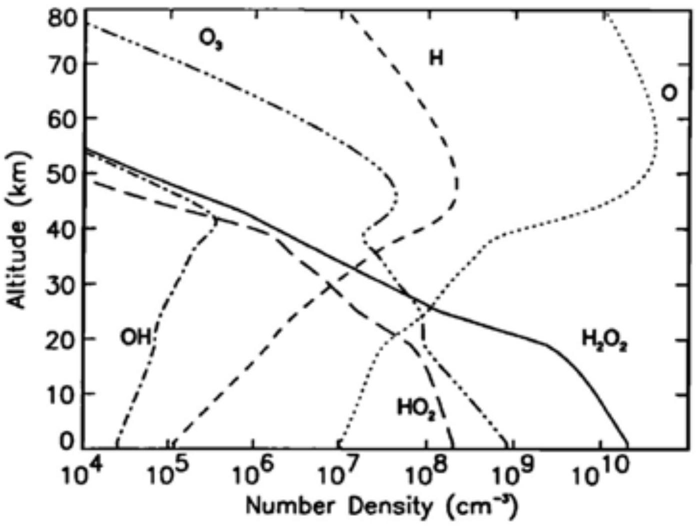

Figure 8. Distribution of key constituents based on the nominal model ($H_2O = 150$ ppm, $K = 10^6\,cm^2 s^{-1}$, $\tau_d = 0.4$; see text).

Photochemistry is effective even near the surface on Mars because of the thin atmosphere.

Catalytic cycle on Venus?

Cl radicals are thought to play crucial roles.

$$\begin{array}{lr}
Cl + CO + M \rightarrow \boxed{ClCO} + M & (27) \\
\boxed{ClCO} + O \rightarrow CO_2 + Cl & (28) \\
\hline
\text{Net: } CO + O \rightarrow CO_2 & (E)
\end{array}$$

$$\begin{array}{lr}
\boxed{Cl} + CO + M \rightarrow \boxed{ClCO} + M & (27) \\
\boxed{ClCO} + O_2 + M \rightarrow \boxed{ClC(O)OO} + M & (29) \\
\boxed{ClC(O)OO} + \boxed{Cl} \rightarrow CO_2 + ClO + \boxed{Cl} & (30) \\
ClO + O \rightarrow \boxed{Cl} + O_2 & (26) \\
\hline
\text{Net: } CO + O \rightarrow CO_2 & (G1)
\end{array}$$

$$\begin{array}{lr}
\boxed{Cl} + CO + M \rightarrow \boxed{ClCO} + M & (27) \\
\boxed{ClCO} + O_2 + M \rightarrow \boxed{ClC(O)OO} + M & (29) \\
\boxed{ClC(O)OO} + O \rightarrow CO_2 + O_2 + \boxed{Cl} & (31) \\
\hline
\text{Net: } CO + O \rightarrow CO_2 & (G2)
\end{array}$$

$$\begin{array}{lr}
\boxed{Cl} + CO + M \rightarrow \boxed{ClCO} + M & (27) \\
\boxed{ClCO} + O_2 + M \rightarrow \boxed{ClC(O)OO} + M & (29) \\
\boxed{ClC(O)OO} + h\nu \rightarrow CO_2 + ClO & (32) \\
ClO + O \rightarrow \boxed{Cl} + O_2 & (26) \\
\hline
\text{Net: } CO + O \rightarrow CO_2 & (G3)
\end{array}$$

Mills et al. (2007)

Mills et al. (2007)

Vega-2 X-ray spectrometer result
(Andreychikov et al. 1987)

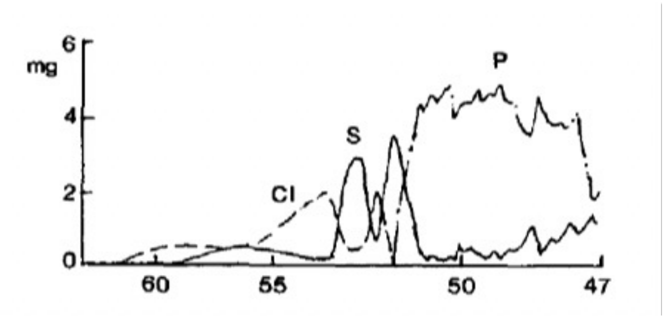

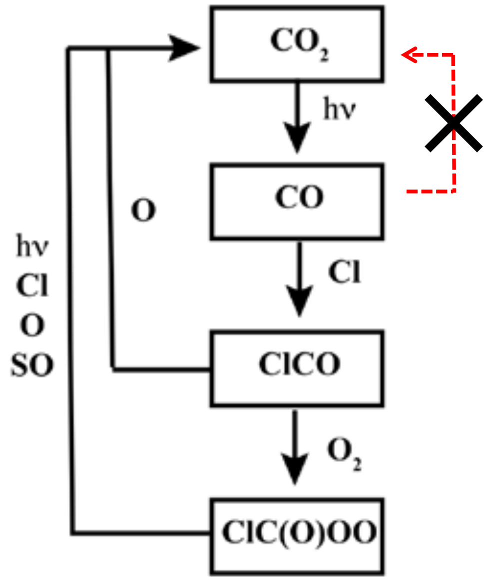

Figure 3. Schematic showing primary pathways for production of CO_2 via chlorine chemistry. The reaction ClCO + O → CO_2 + Cl accounts for 15 and 20% of the column total CO_2 production in the +0.5σ and +2.0σ models from Table 5, respectively.

ClCO, $ClCO_3$ and other key species have never been observed.

Clouds/aerosols

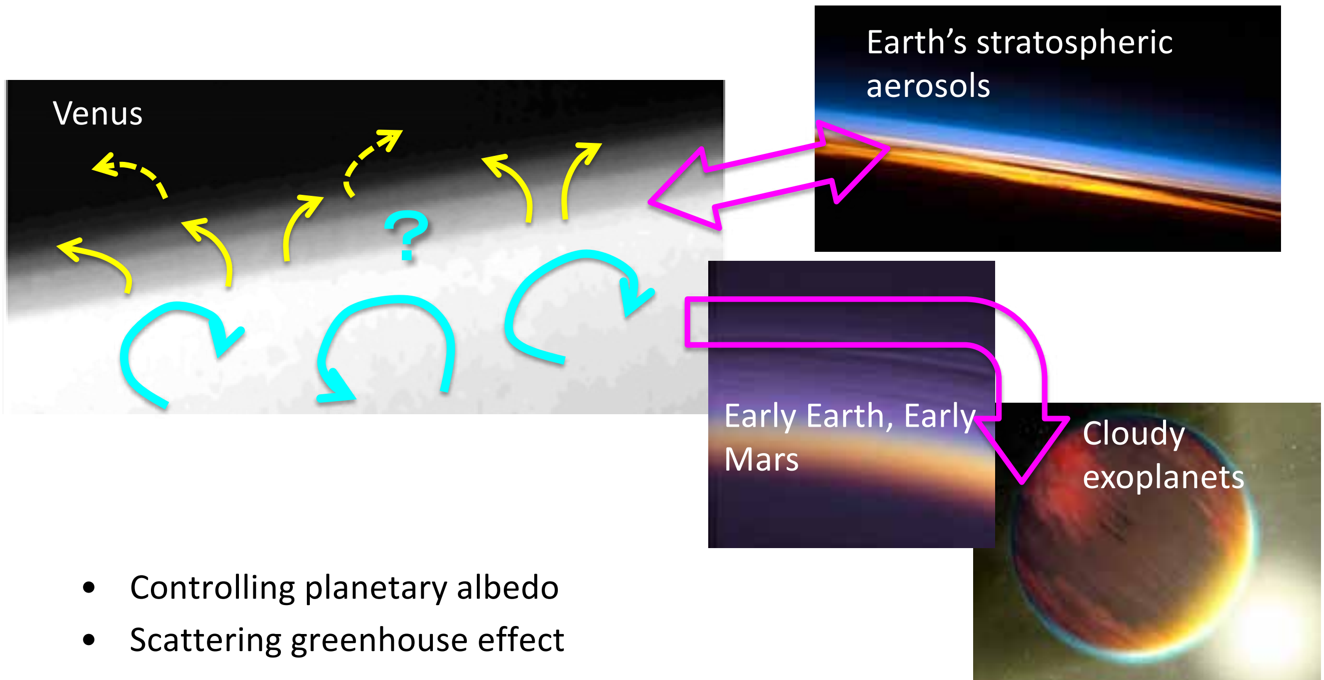

- Controlling planetary albedo
- Scattering greenhouse effect
- Regulating atmospheric species transported to the upper atmosphere

Cloud formation

Andrews (2010)

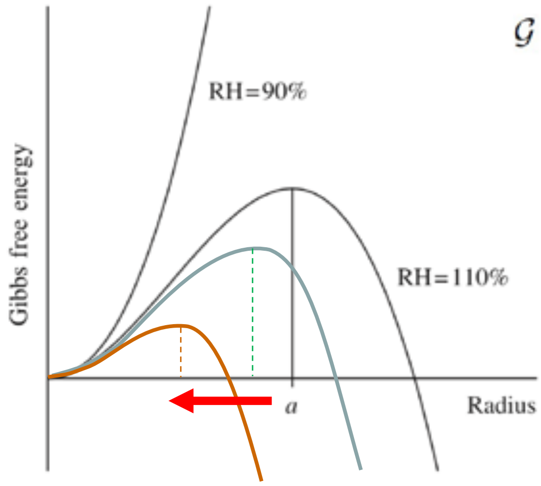

Gibbs free energy

$$\mathcal{G} - \mathcal{G}_0 = -\frac{4}{3}\pi a^3 \rho_l R_v T \ln\left(\frac{e}{e_s(T)}\right) + 4\pi a^2 \gamma$$

a : radius of droplet
e : partial vapor pressure
e_s : saturation vapor pressure
γ : surface tension
ρ_l : liquid density
R_v : gas constant
T : temperature

Pure water:

equilibrium radius	relative humidity(RH)
0.01 µm	→ 112%
0.1 µm	→ 101%
flat surface	→ 100%

If a cloud droplet is to survive, it must somehow attain a radius greater than the equilibrium radius a corresponding to the ambient relative humidity
→ Need for condensation nucleus

Cloud condensation nuclei (CCN)

Example of the composition of ice forming nuclei in Earth's troposphere (Pruppacher & Klett 1997)

TABLE 9.6
Composition of ice forming nuclei derived from aerosolized soil in Montana (from Rosinski *et al.*, 1981).

Chemical composition	Aerosol particles number	Aerosol particles %	Ice-forming nuclei active at temperature −12°C number	−12°C %	−15°C number	−15°C %	−20°C number	−20°C %
Clay minerals:								
montmorillonite	194	24	28	18	17	13	41	28
feldspar	287	36	74	48	41	32	54	38
illite	163	20	37	24	39	31	28	19
miscellaneous	27	3	8	5	19	15	10	7
Organic particles	139	17	7	5	12	9	11	8
Number of particles: analyzed	810		154		128		144	
Mixed particles containing:								
NaCl	7		14	9	28	22	21	15
CuX	2		1		0		1	
$FeO_x.nH_2O$	-		7	5	12	9	11	8
Total	9		22	14	40	31	33	23

- The characteristics of CCN on other planets are mostly unknown.
- Dust particles will serve as CCN on Mars.
- Galactic cosmic rays may also work. Cosmic rays increase small ions (charged molecules or charged small clusters of molecules) in the atmosphere, leading to increase in the nucleation rate of aerosol particles.

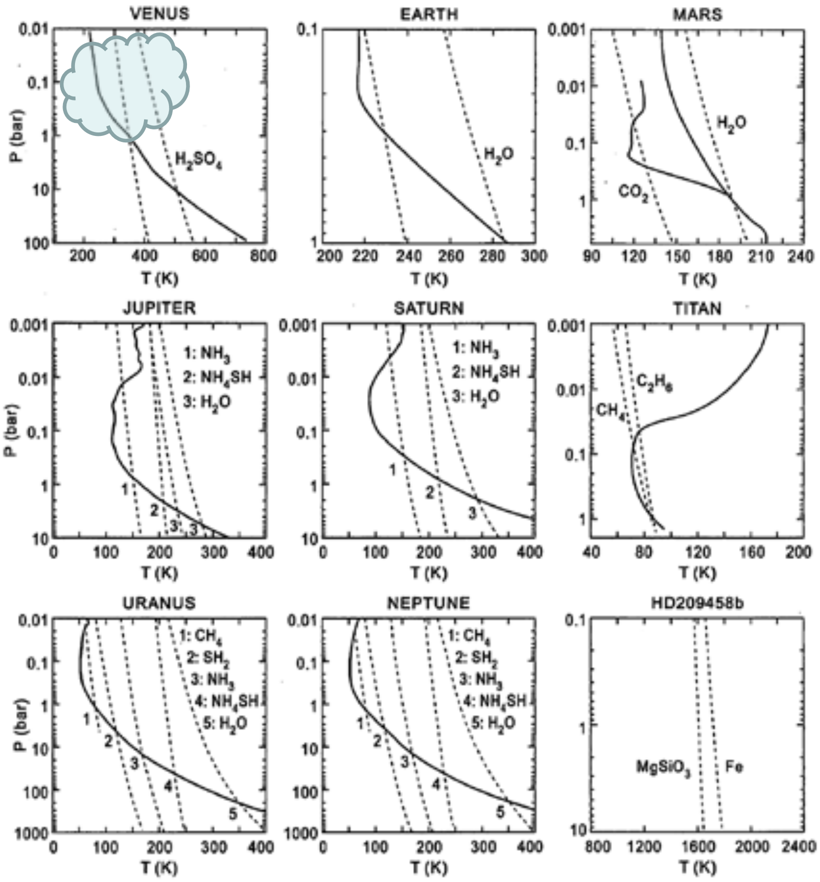

Catling & Kasting (2017)

The solid curves are the typical vertical profiles of pressure versus temperature. Dashed curves are the saturation vapor pressure curves for various condensables.

Particles condense when the partial pressure reaches the saturation vapor pressure.

H_2SO_4 clouds of Venus

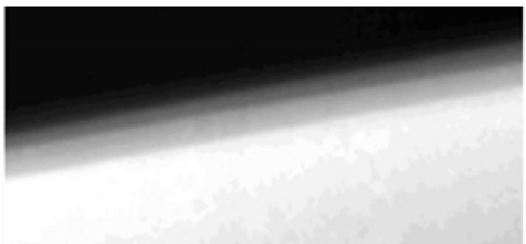

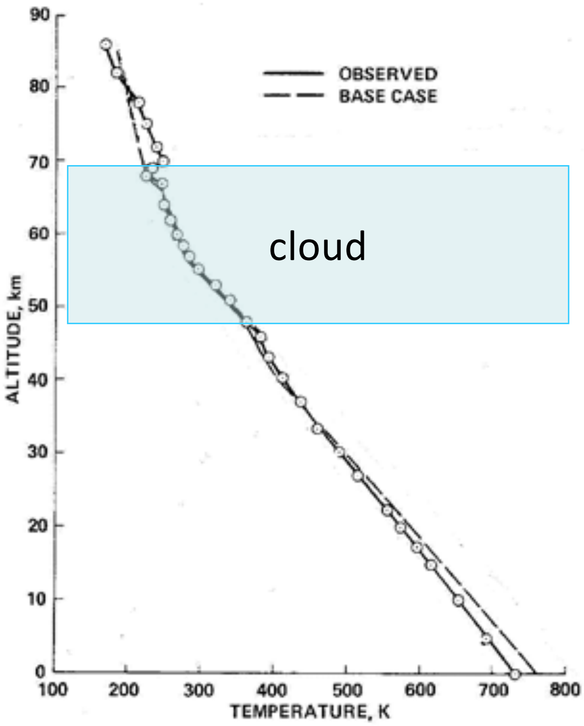

Fig. 2. Comparison between the observed temperature structure of Venus' lower atmosphere and that of several models, which are described in the main text.

- Solar energy flux reaching the Venus surface (17W/m^2) is much less than that of the Earth (168W/m^2).
- Greenhouse effect of massive CO_2 and small amount of H_2O explains the high temperature.

Pollack et al. (1980)

Microphysical properties of Venus clouds

- H_2SO_4-H_2O droplets with radii r < 5 μm
- Smallest mode (including sub-cloud haze) might be condensation nuclei whose composition is unknown.
- Size distribution is variable.

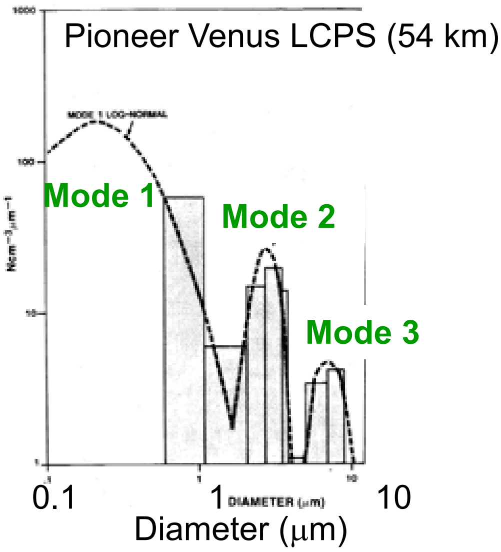

Venera-13 Lander

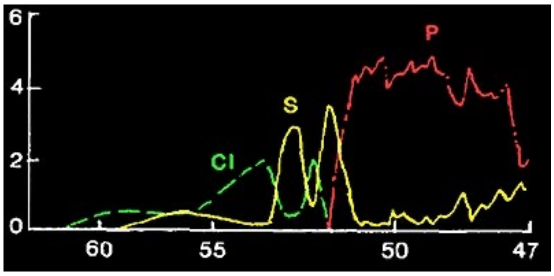

Cl ? S ? P ?

Origin of clouds

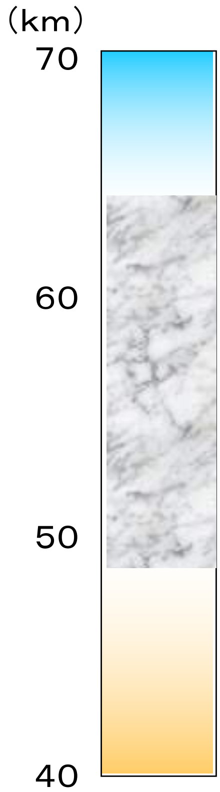

Photochemistry above clouds

Scenario #1 (Net reaction driven by catalytic cycles including ClOx, HOx, NOx)

$2CO_2 + h\nu \rightarrow 2CO + O_2$

$CO + SO_2 + O_2 + h\nu \rightarrow CO_2 + SO_3$

$CO_2 + SO_2 + h\nu \rightarrow CO + SO_3$

Scenario #2

$SO_2 + h\nu \rightarrow SO + O$

$SO + h\nu \rightarrow S + O$

$SO_2 + O \rightarrow SO_3$ (×2)

$3\,SO_2 + h\nu \rightarrow S + 2SO_3$

- SO_3 rapidly reacts with H_2O: $SO_3 + H_2O \rightarrow H_2SO_4$
- Elemental sulfur (S) can serve as condensation nuclei.

Origin of clouds

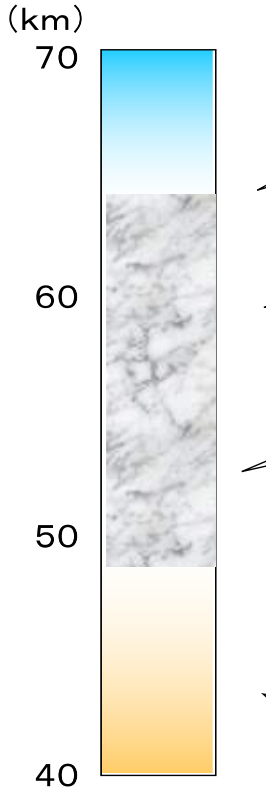

H_2SO_4 vapor and H_2O vapor condenses onto condensation nuclei.

Growth of particles via collision during gravitational sedimentation

Evaporation around 50 km altitude due to high temperature

Thermochemistry below clouds (Net reaction driven by catalytic cycles

$H_2SO_4 \rightarrow H_2O + SO_3$

$SO_3 + CO \rightarrow CO_2 + SO_2$

$SO_3 + OCS \rightarrow CO_2 + (SO)_2$ etc

$H_2SO_4 + 4CO \rightarrow H_2O + 3CO_2 + OCS$

Sedimentation of particles

Stokes velocity for a spherical particle

$$w_{\mathrm{sed}} = \frac{g\rho d^2}{18\eta}$$

g : gravitational acceleration

ρ : mass density of particle

d : diameter of particle

η : viscosity coefficient of air

comparable

Time constant of Hadley circulation

τ ~ 100 Earth days (from energy budget)

→ Vertical flow velocity ~ H/τ ~ 1 mm/s

Sedimentation velocity of droplets in Venusian atmosphere
(Imamura & Hashimoto 1998)

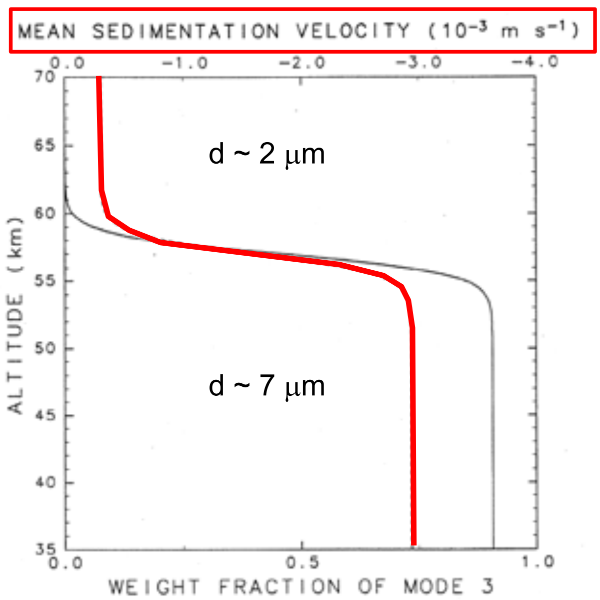

Figure 2. Fraction of Mode 3 particles by weight in the cloud (solid curve) adopted in the model after the observation by the Pioneer Venus particle size spectrometer, and the calculated mean sedimentation velocity W_{sed} (dashed curve). The cloud mass is assumed to be composed of particles of fixed radii, Mode 2 ($r = 1.15$ μm) and Mode 3 ($r = 3.65$ μm).

Possible role of planetary-scale meridional circulation

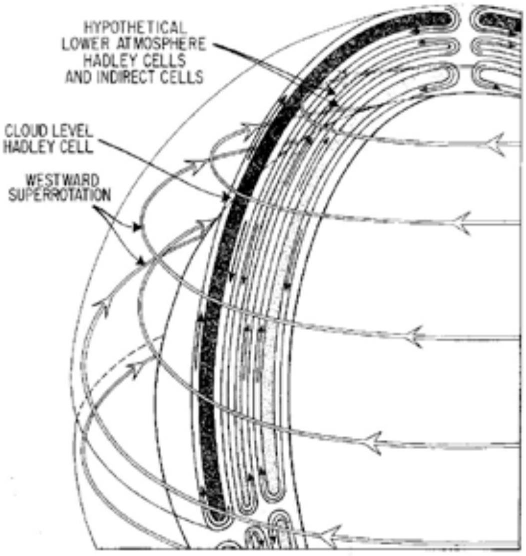

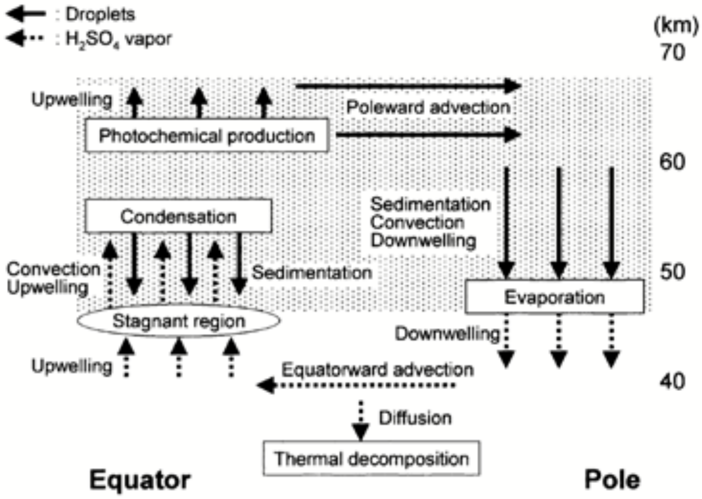

Schubert (1983)

Imamura & Hashimoto (2001)

Lifecycle of Earth's stratospheric aerosols

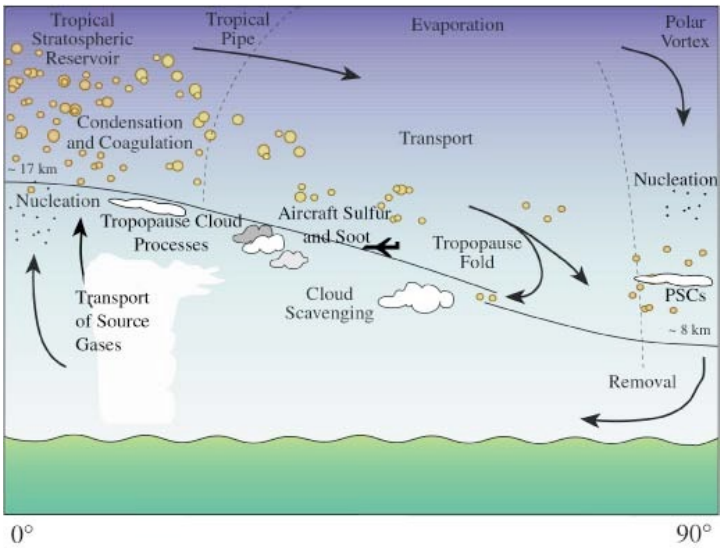

Hamill et al. (1997)

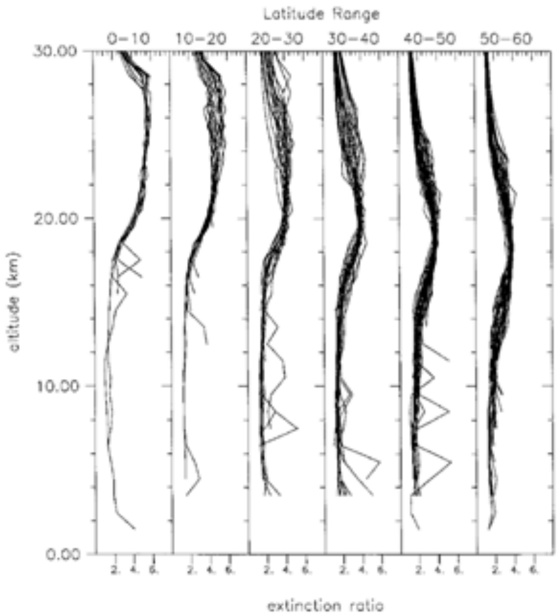

FIG. 9. Extinction ratios from the SAGE II satellite system in various latitude ranges. The extinction values were measured in April 1989 in the Southern Hemisphere. We have removed extinction ratios greater than 7 at lower altitudes for these are indications of tropospheric clouds.

SO_2 (283 nm)

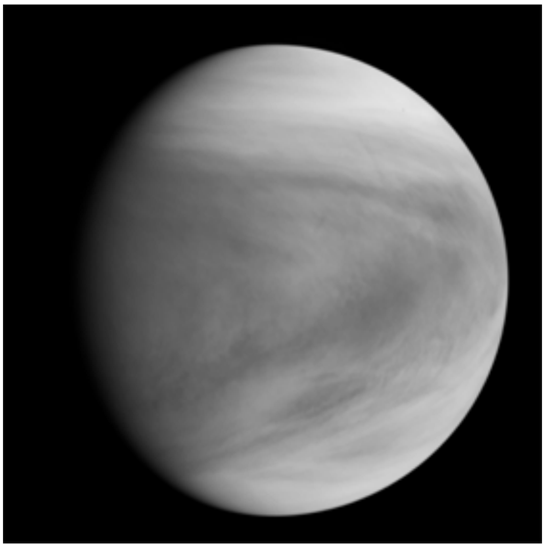

Unknown absorber (365 nm)

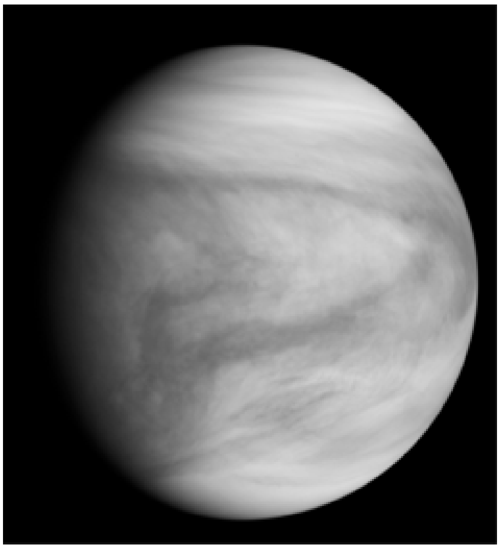

Venus is completely covered by clouds that are featureless in the visible but exhibit variable ultraviolet features.

Origin of visible-UV absorption

- Absorbing material at far UV (<320nm) is mostly SO_2
- Absorption at near UV (>320nm) is a mystery. Candidate species are S_X, S_2O_2, S_2O, $FeCl_2$, etc.
- Cause of the yellowish color of Venus

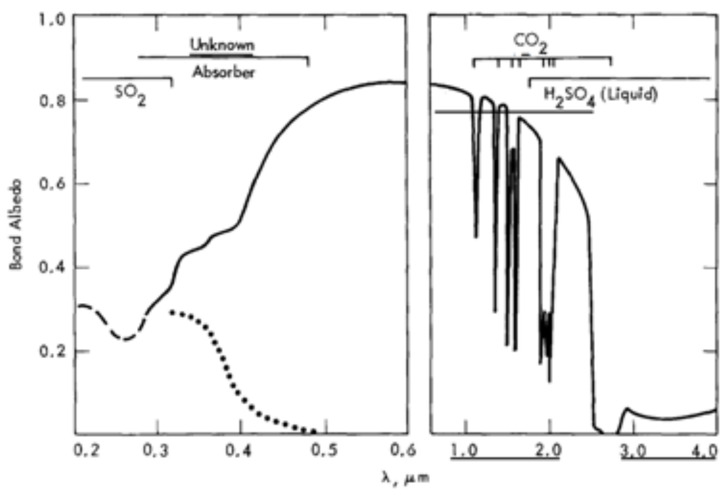

Moroz et al. (1985)

Figure 6-1. The Monochromatic Bond Albedo of Venus as a Function of Wavelength (Moroz, 1983 - Normalized to the Integrated Albedo A = 0.76). The points show the wavelength dependence of the maximum contrast between dark and light UV features (Coffeen, 1977).

Dust in the Martian atmosphere

- Micrometer-sized small mineral particles float in the atmosphere with a background optical thickness of 0.1–0.5.
- The dust loading changes with time and space.
- The dust serves as a heat source in the atmosphere by absorbing sunlight.

Martian dust storms span the entire planet, in June 2018. The image was taken from the NASA's rover *Curiosity*

Seasons of Mars

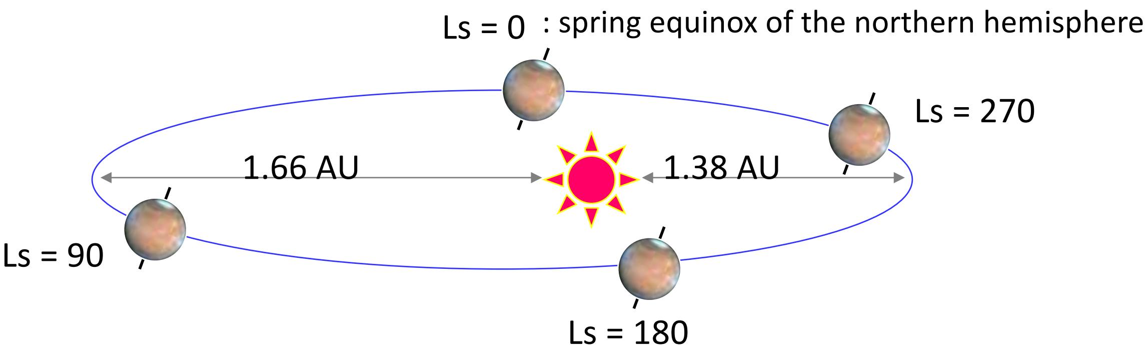

- The north-south asymmetry of the seasonal cycle is large due to the large orbital eccentricity.
- The distance to the sun gets closer in the southern summer.

Dust storms on Mars

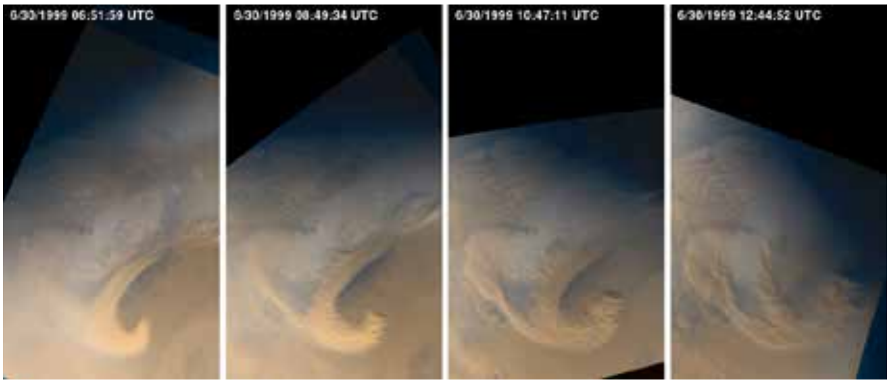

regional storm

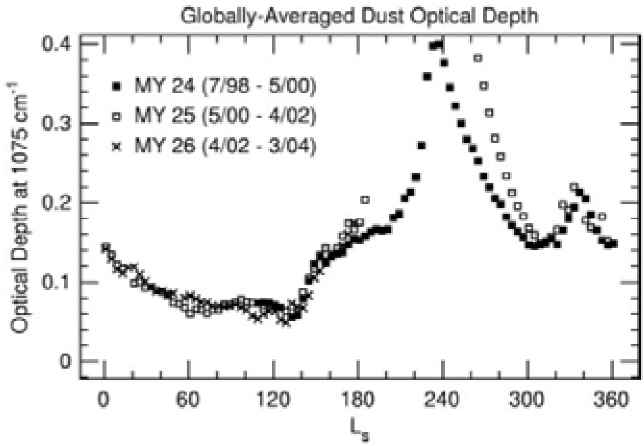

Seasonal variation of optical thickness in infrared
(Smith et al. 2004)

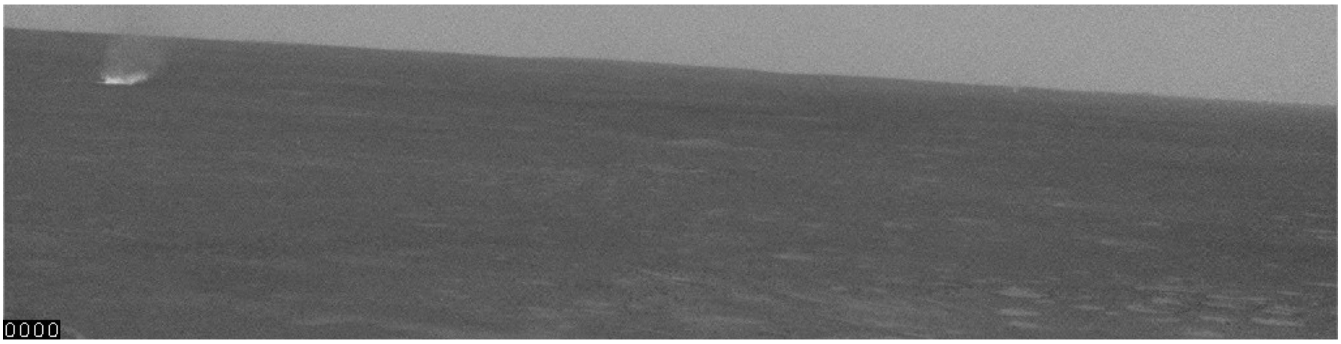

Dust devils

- Source of background atmospheric dust ?

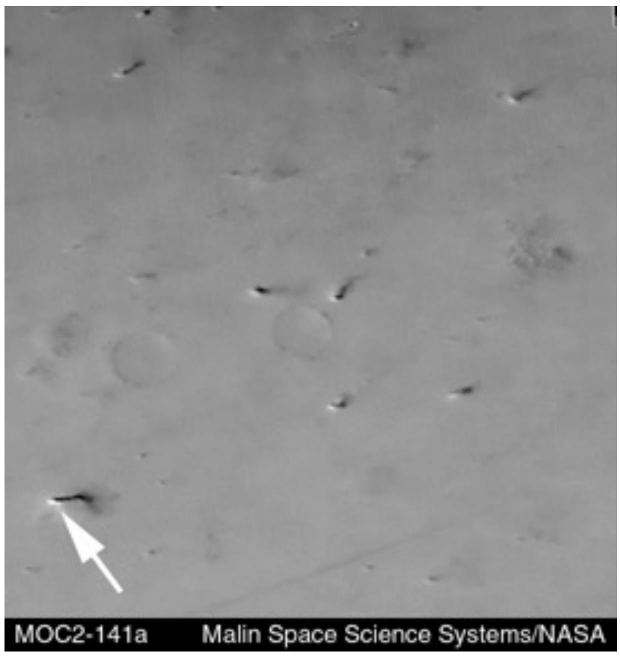

H_2O ice clouds on Mars

HST Mars image

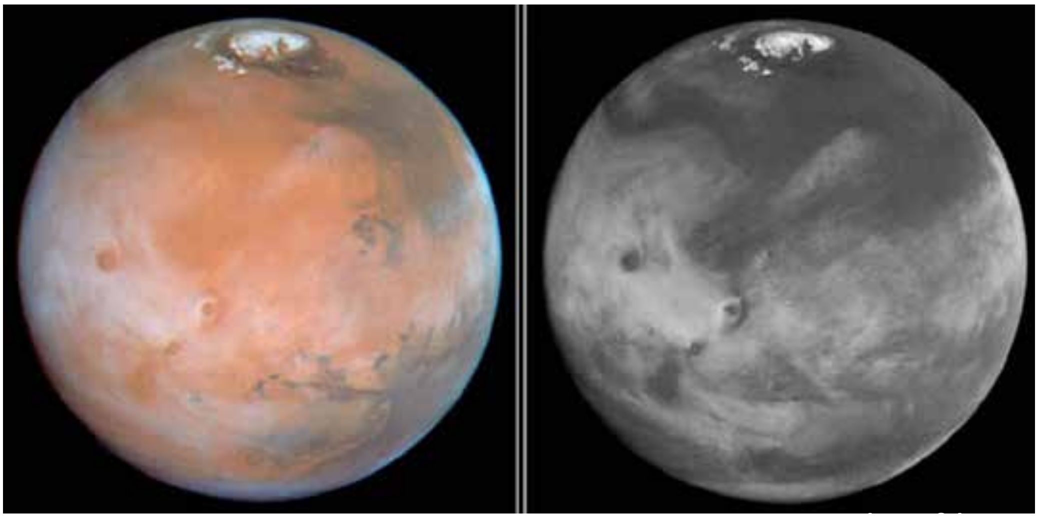

color composite blue (410 nm)

Seasonal variation of dust, clouds, and H_2O vapor observed by an infrared spectrometer (TES) on Mars Global Surveyor

Dust

Ice clouds

Water vapor

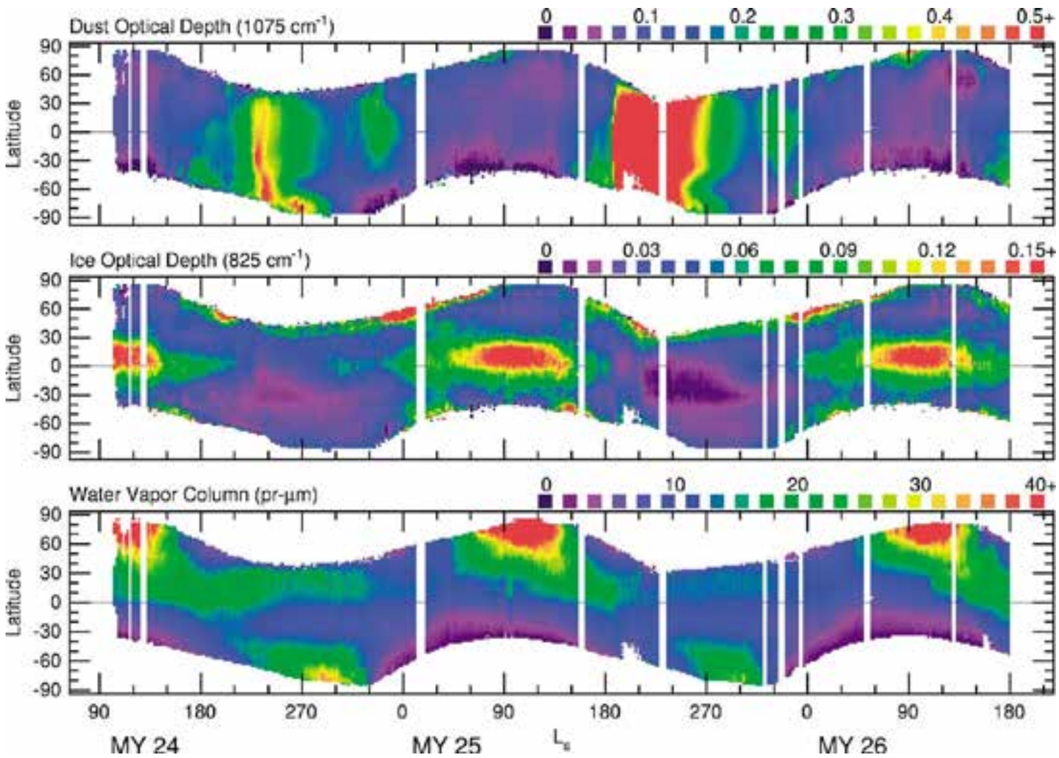

Smith, Icarus 167 (2004) 148–165

Supersaturation of water vapor on Mars

SPICAM on Mars Express (Maltagliati et al. 2011)

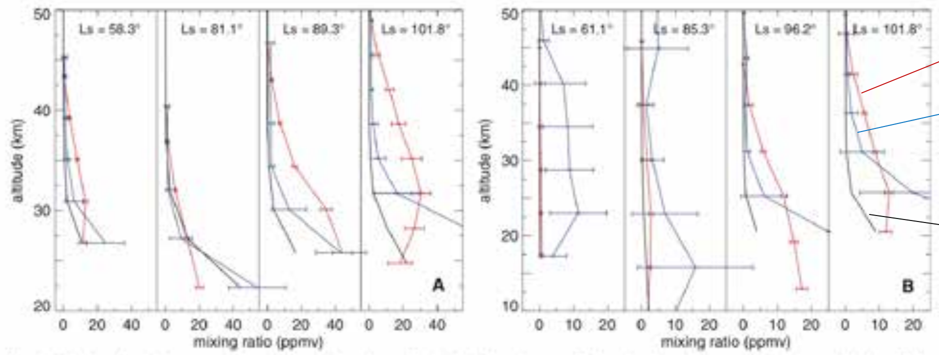

Observation

Saturation pressure

Model

Fig. 2. Selection of typical water vapor volume–mixing ratio profiles in the (**A**) northern and (**B**) southern hemisphere. Black curve, modeled profile by the LMD-GCM; red curve, the retrieved SPICAM results; blue curve, saturation water vapor–mixing ratio. Supersaturation exists where the red values are greater than the blue ones.

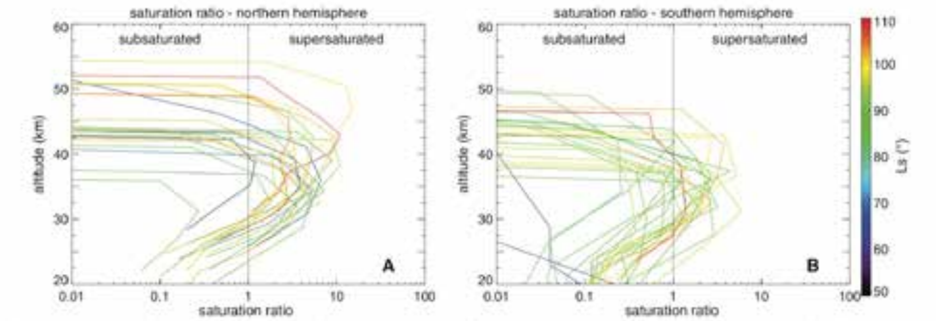

Fig. 3. Saturation ratio for all orbits of the campaign. (**A**) Northern hemisphere. (**B**) Southern hemisphere. The vertical line marks the value of 1, which corresponds to the saturated state.

Dependence of volatile escape on lower atmosphere processes

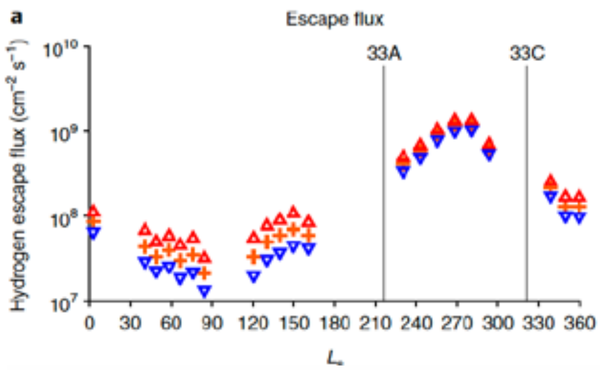

Hydrogen escape measured by MAVEN Solar Wind Ion Analyzer

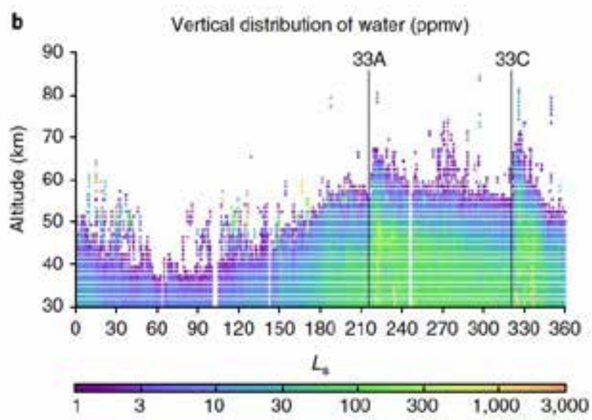

Vertical distribution of total water content measured by MRO MCS

Heavens et al. (2018)

Meridional cross sections in Mars GCM
(Shaposhnikov et al. 2019)

Meridional distribution of zonal-mean temperature obtained by MGS/TES
(Smith et al. 2001)

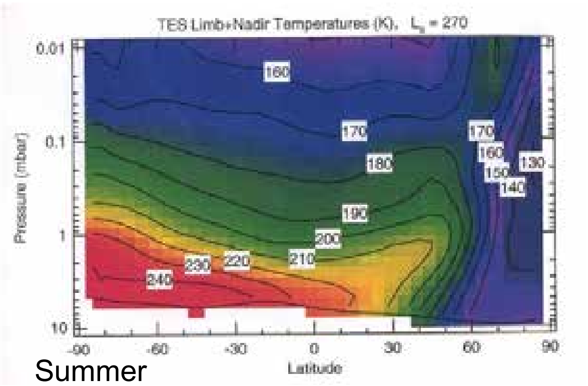

Summer
Winter

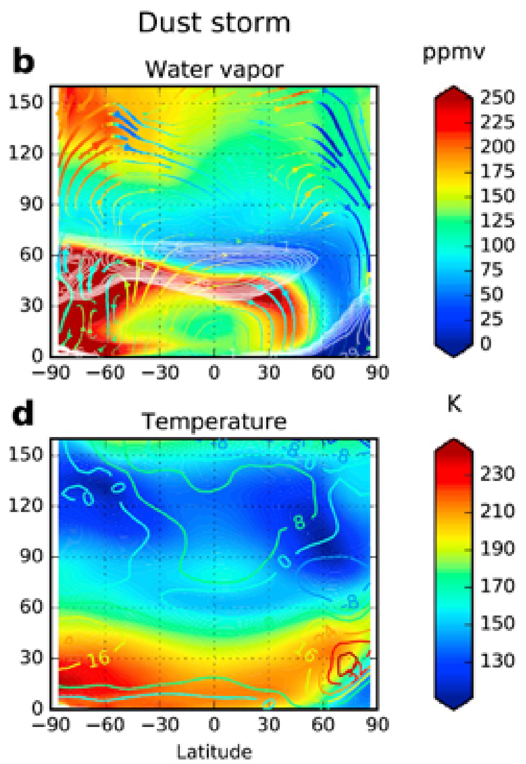

Traditional scheme

New concept

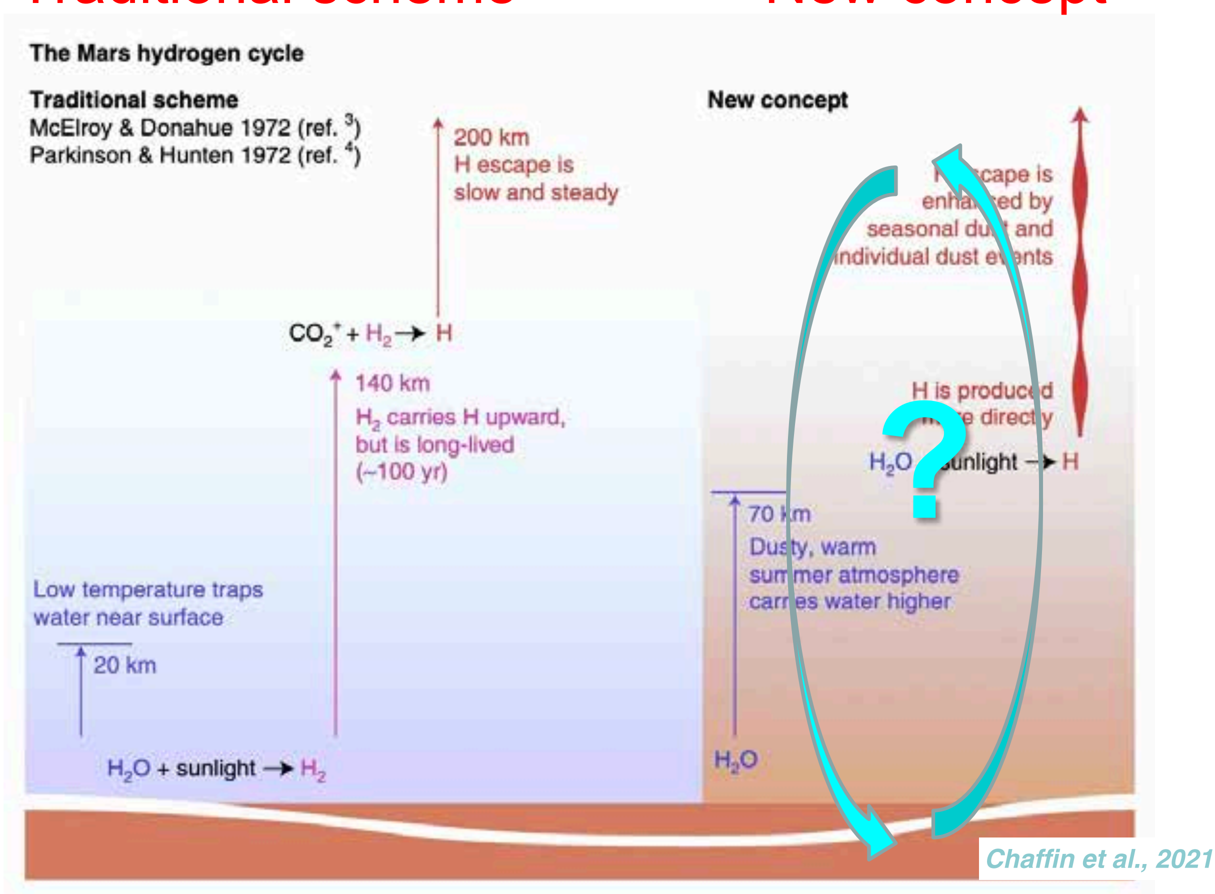

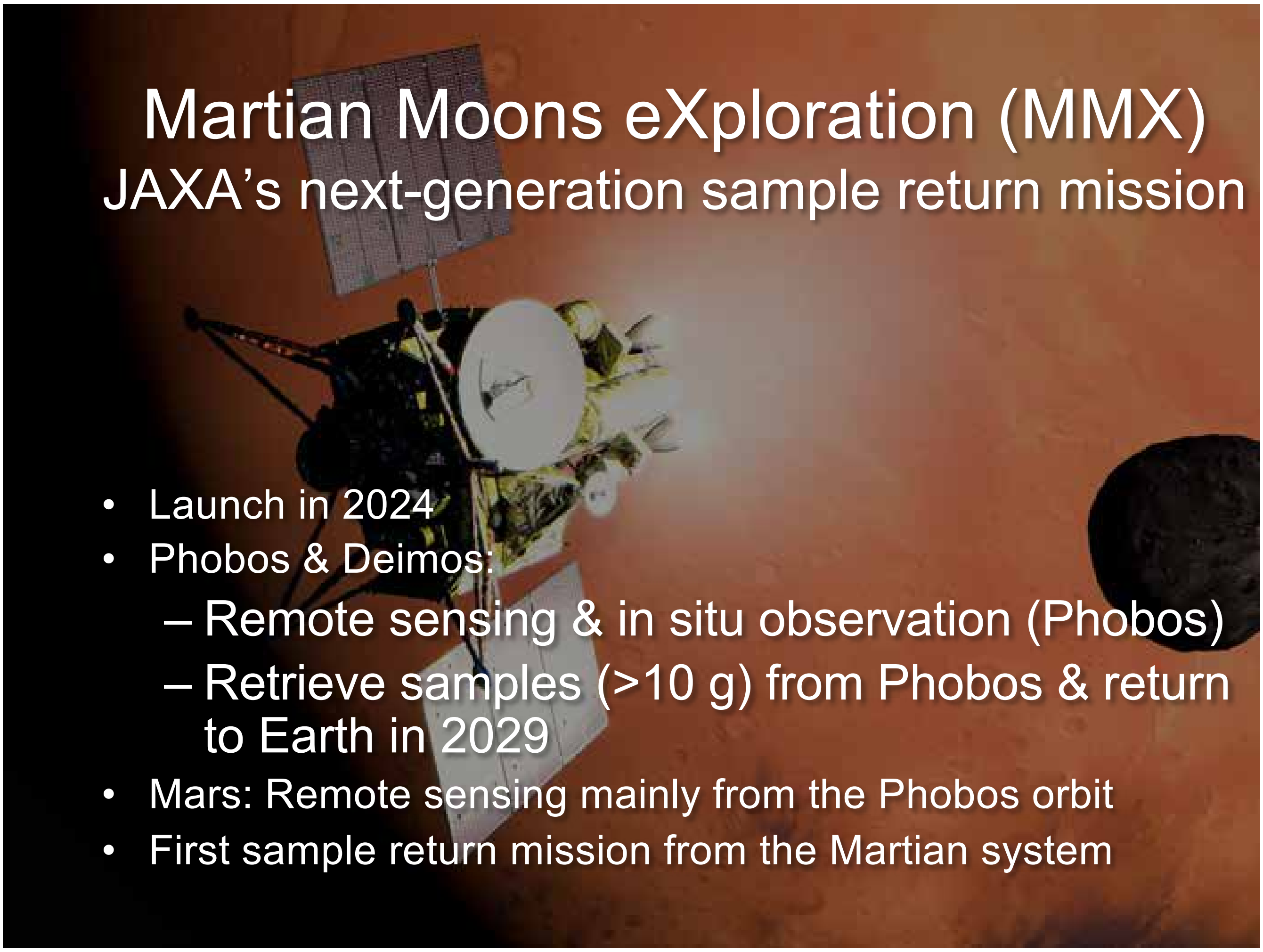

Martian Moons eXploration (MMX)

JAXA's next-generation sample return mission

- Launch in 2024
- Phobos & Deimos:
  – Remote sensing & in situ observation (Phobos)
  – Retrieve samples (>10 g) from Phobos & return to Earth in 2029
- Mars: Remote sensing mainly from the Phobos orbit
- First sample return mission from the Martian system

Instruments for Mars atmosphere observation

- **OROCHI**
  – Wide-angle camera, 8 colors
  – 3 colors (480, 650, 950 nm) will be used for Mars observation.
  – 2.5 km/pix (sub S/C) from QSO
- **TENGOO**
  – Narrow-angle camera
  – 35 m/pix (sub S/C) from QSO
- **MIRS**
  – Push-bloom type spectrometer
  – Spectral resolution: 10nm
  – Spectral bandpass: 0.9–3.6 μm
  – 2.1 km/pix (sub S/C) from QSO

Kameda et al. (2021)

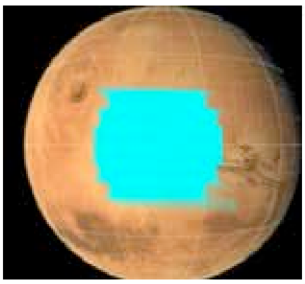

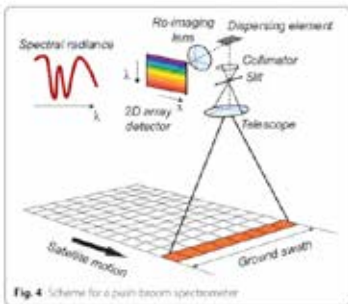

Barucci et al. (2021)

Continuous global monitoring from Martian orbit

High-altitude equatorial orbit is a unique platform for atmospheric studies

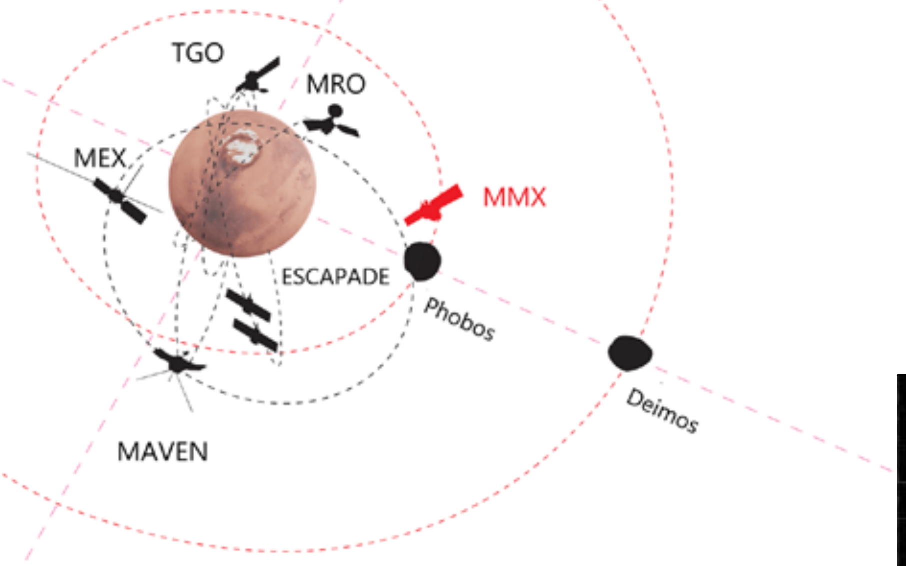

Ogohara et al. (2022)

Venus images taken by JAXA's Akatsuki

UV

IR

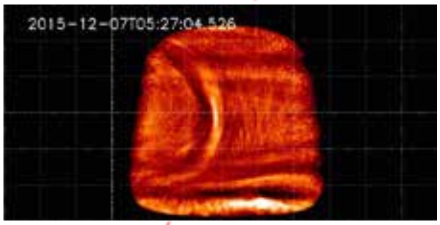

Chemistry of gas giants

Thermodynamically stable hydrides: CH_4, NH_3, H_2O, H_2S, PH_3, GeH_4, AsH_3 ...

These gases (except H_2O and H_2S) are photochemically destroyed by solar UV to produce disequilibrium species, such as ethane C_2H_6, ethylene C_2H_4, acetylene C_2H_2, hydrazine N_2H_4.

The disequilibrium species react with H_2 to reform hydrides once they are transported downward into the hot, high pressure regions.

Lodders, 2010

Table 2. *Composition of the Atmospheres of Jupiter, Saturn, Uranus, and Neptune*

Gas	Jupiter[a]	Saturn	Uranus	Neptune
H_2	86.4 ± 0.3%	88 ± 2%	~82.5 ± 3.3%	~80 ± 3.2 %
^4He	13.6 ± 0.3%	12 ± 2%	15.2 ± 3.3 %	19.0 ± 3.2 %
CH_4	$(1.81 \pm 0.34) \times 10^{-3}$	$(4.7 \pm 0.2) \times 10^{-3}$	~2.3 %	~1-2 %
NH_3	$(6.1 \pm 2.8) \times 10^{-4}$	$(1.6 \pm 1.1) \times 10^{-4}$	<100 ppb	<600 ppb
H_2O	520^{+340}_{-240} ppm	2–20 ppb		
H_2S	67 ± 4 ppm	<0.4 ppm	<0.8 ppm	<3 ppm
HD	45 ± 12 ppm	110 ± 58 ppm	~148 ppm	~192 ppm
$^{13}CH_4$	19 ± 1 ppm	51±2 ppm		
C_2H_6	5.8 ± 1.5 ppm	7.0 ± 1.5 ppm		
PH_3	1.1 ± 0.4 ppm	4.5 ± 1.4 ppm		
CH_3D	0.20 ± 0.04 ppm	0.30 ± 0.02 ppm	~8.3 ppm	~12 ppm
C_2H_2	0.11 ± 0.03 ppm	0.30 ± 0.10 ppm	~10 ppb	60^{+140}_{-40} ppb
HCN	60 ± 10 ppb	<4 ppb	<15 ppb	0.3 ± 0.15 ppb
HC_3N			<0.8 ppb	<0.4 ppb
C_2H_4	7 ± 3 ppb	~0.2 ppb[b]		
CO_2	5-35 ppb	0.3 ppb	40 ± 5 ppt	
C_2H_6			10 ± 1 ppb	$1.5^{+2.5}_{-0.5}$ ppm
CH_3C_2H	2.5^{+2}_{-1} ppb	0.6 ppb	0.25 ± 0.03 ppb	
CO	1.6 ± 0.3 ppb	1.4 ± 0.7 ppb	<40 ppb	0.65 ± 0.35 ppm
CH_3CN				<5 ppb
GeH_4	$0.7^{+0.4}_{-0.2}$ ppb	0.4 ± 0.4 ppb		
C_4H_2	0.3 ± 0.2 ppb	0.09 ppb	0.16 ± 0.02 ppb	
AsH_3	0.22 ± 0.11 ppb	2.1 ± 1.3 ppb		

[a] ^3He 22.6±0.7 ppm, Ne 21±3 ppm, Ar 16±3 ppm, Kr 8±1 ppb, Xe 0.8±0.1 ppb.
[b]assuming a total stratospheric column density of 1.54%10^{25} cm^{-2}.
From Lodders & Fegley 1998 and updates: Mahaffy et al. 2000, Atreya et al. 2003, Lodders 2004, Wong et al. 2004

Chemical cycle of hydrogen-bearing species in giant planets

Catling & Kasting (2017)

$$2CH_4 + \text{photons} \rightarrow \underbrace{C_2H_6 + H_2}_{\text{ethane + hydrogen}}$$

$$2nCH_4 + \text{photons} \rightarrow \underbrace{(C_2H_2)_n + 3nH_2}_{\text{polyacetylene + hydrogen}}$$

$$6nCH_4 + \text{photons} \rightarrow \underbrace{(C_6H_6)_n + 9nH_2}_{\text{polyaromatic hydrocarbons + hydrogen}}$$

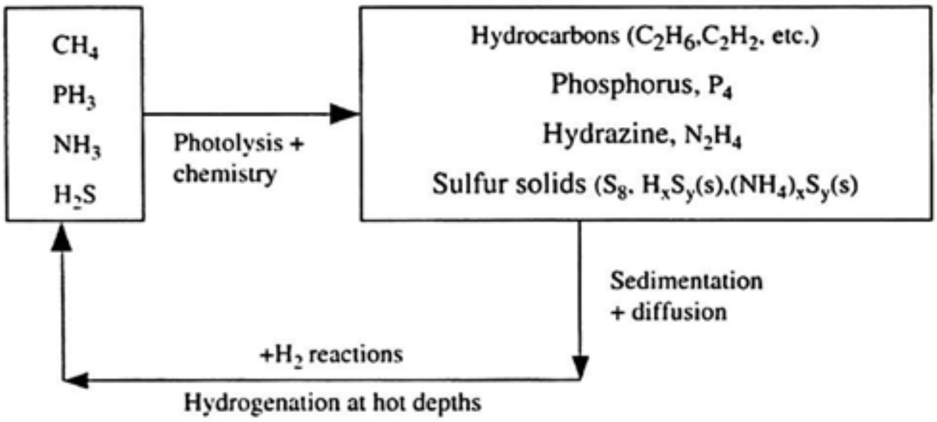

Clouds of Jupiter and Saturn

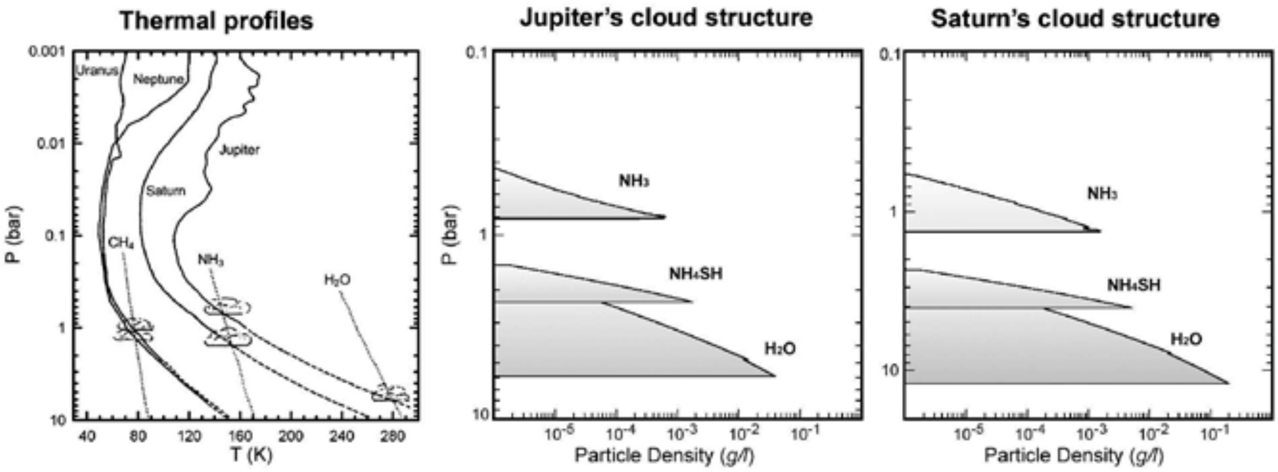

Sanchez-Lavega et al.

Atmospheric chemistry on Titan

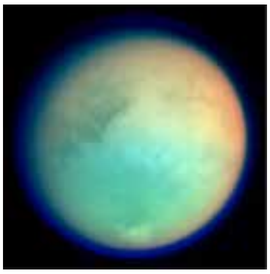

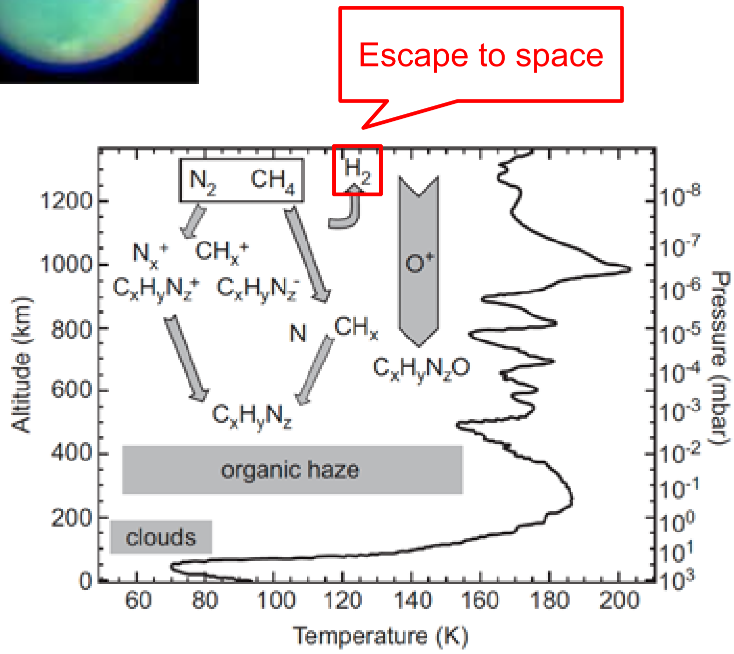

Vuitton et al. (2014)

Atmospheric composition of Titan (Coustenis 2007)

Constituent	Mole Fraction (atm. altitude level)
Major	
Molecular nitrogen, N_2	0.98
Methane, CH_4	4.9×10^{-2} (surface)
	$1.4–1.6 \times 10^{-2}$ (stratosphere)
Monodeuterated methane, CH_3D	6×10^{-6} (in CH_3D, in stratosphere.)
Argon, ^{36}Ar	2.8×10^{-7}
^{40}Ar	4.3×10^{-5}
Minor	
Hydrogen, H_2	~0.0011
Ethane, C_2H_6	1.5×10^{-5} (around 130 km)
Propane, C_3H_8	5×10^{-7} (around 125 km)
Acetylene, C_2H_2	4×10^{-6} (around 140 km)
Ethylene, C_2H_4	1.5×10^{-7} (around 130 km)
Methylacetylene, CH_3C_2H	6.5×10^{-9} (around 110 km)[a]
Diacetylene, C_4H_2	1.3×10^{-9} (around 110 km)[a]
Cyanogen, C_2N_2	5.5×10^{-9} (around 120 km)[a]
Hydrogen cyanide, HCN	1.0×10^{-7} (around 120 km)[a]
	5×10^{-7} (around 200 km)[b]
	5×10^{-6} (around 500 km)[b]
Cyanoacetylene, HC_3N	1×10^{-9} (around 120 km)[a]
	1×10^{-7} (around 500 km)[b]
Acetonitrile, CH_3CN	1×10^{-8} (around 200 km)[f]
	1×10^{-7} (around 500 km)
Water, H_2O	8×10^{-9} (at 400 km)[d]
Carbon monoxide, CO	4×10^{-5} (uniform profile)[e]
Carbon dioxide, CO2	1.5×10^{-8} (around 120 km)

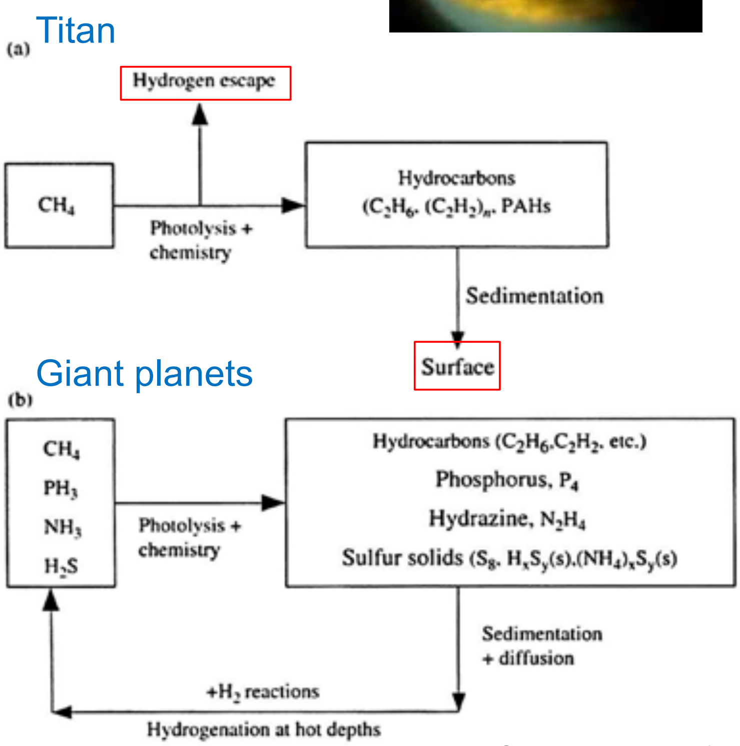

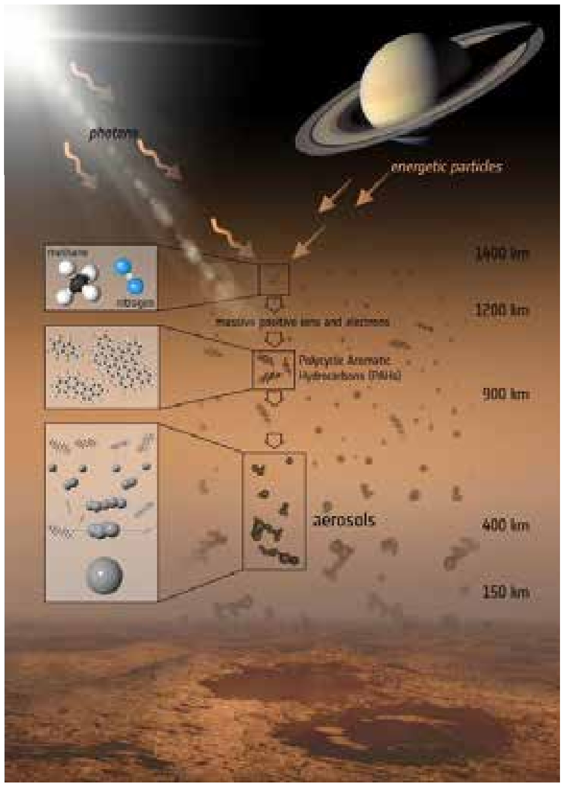

© NASA

Catling & Kasting (2017)

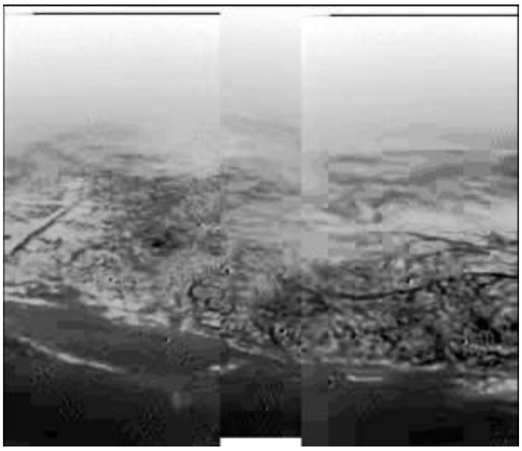

Huygens’ touchdown

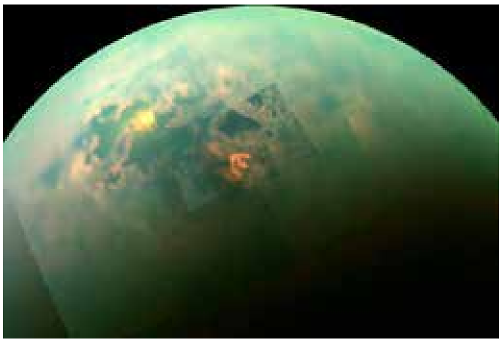

Cassini's Visual and Infrared Mapping Spectrometer (VIMS)